EMISSION AND ABSORPTION OF CYCLOTRON
RADIATION BY A HOT ELECTRON PLASMA

by

S. Sesnic, D. Tuma, A. J. Lichtenberg
and A. W. Trivelpiece

ELECTRONICS RESEARCH LABORATORY

College of Engineering
University of California, Berkeley
94720

Manuscript submitted: 26 August 1966

ABSTRACT

The <u>absolute</u> spectral intensity of the synchrotron radiation emitted from a hot electron plasma in a strong magnetic field has been measured in the 4.0 to 0.2 mm wavelength range. The spectral distribution of this radiation, for propagation perpendicular and parallel to the magnetic field, is in general agreement with the theoretical predictions of Trubnikov and others, based on independent emission from a two-dimensional Maxwellian distribution of single particles. Both the temperature and density of the plasma have been determined from these measurements. The radiation spectrum exhibits some additional structure which has not been completely explained. Measurements have also been made, with a broadband detector, of the total time-resolved radiation. In addition to yielding similar values of temperature and density, these broadband measurements proved to be a convenient method of observing instabilities.

The absorption of microwave energy, both at cyclotron resonance and at other values of magnetic field, has been studied with 3 cm and 8 mm magnetron pulses. In contrast to other microwave heating experiments, the plasma parameters were such that the interaction was primarily with single electrons. The results, which agree qualitatively with analytical and numerical calculations, show no significant heating of the main body of the plasma, although a few electrons are given large increases in energy. In some instances, the microwave radiation pulses could induce instabilities in the confined plasma.

INTRODUCTION

In this paper we report the results of experiments for studying the emission and absorption of electromagnetic radiation by a magnetically confined "hot electron" plasma. The hot electron plasma is created in the single stage, magnetic mirror, compression experiment[1] depicted schematically in Fig. 1. The plasma is generated by a deuterated titanium washer stack source,[2] which injects plasma into the magnetic mirror field during the initial period of the compression cycle. A portion of the plasma injected from the source is trapped and compressed in the mirror field. The mirror ratio is 1.5:1, the rise time is 500 μsec, and the field decay time constant is 25 msec. The maximum midplane magnetic field for most of the experiments reported here was 50 kG; however, experiments were conducted over a range of magnetic fields from 30 to 60 kG.

For a 50-kG peak field, the plasma has an electron temperature measured by X-ray pulse height analysis, of between 75 and 80 keV, a density of approximately $10^{12}/cm^3$ and may be stable with a decay constant of a few milliseconds. The diameter of the plasma at peak compression is measured to be 4 - 6 mm, and the length is estimated to be about 3 cm. The plasma temperature is determined by comparing the measured, single X-ray pulse-height distribution, obtained from a series of shots, with the computed distribution function for a

two-dimensional Maxwellian distribution. The variation in temperature from one pulse-height measurement to another is less than 5%. The dimensions and location of the plasma are determined by means of a plasma camera, which is an 8-cm diameter quartz flat, coated with aluminized (10 keV thick) P-11 phosphor. The quartz flat is situated perpendicular to the magnetic axis outside the mirror peak so as to intercept end-loss electrons. An image-converter camera with a 100-μsec shutter time is used to photograph the back of the quartz flat.

For frequencies much higher than the plasma frequency, the real part of the index of refraction of a plasma is nearly unity. For this situation Trubnikov,[3] and Drummond and Rosenbluth[4] show that collective interactions between the plasma particles have a negligible effect on the absorption and emission of radiation. This implies that the emission and absorption properties of a high-temperature, tenuous plasma, such as used in the experiments reported here, can be obtained from single particle theory assuming an optically thin plasma. We outline the single particle theory, applicable to our experimental investigation, here. This theory will be compared with the experimental results in Secs. II and III.

A. Radiation

In a steady magnetic field, an electron moves along a helical path. As a result of this motion, the electron radiates electromagnetic

energy at its cyclotron frequency and harmonics, where the Doppler-shifted cyclotron frequency of the radiation in the direction of observation is given by

$$\omega_c = eB/m_0 \gamma(1 - \beta_\| \cos \theta) \,, \qquad (1)$$

The angle of observation θ is measured from the magnetic axis; $\beta_\| = v_\|/c$ and $\beta_\perp = v_\perp/c$ are the normalized parallel and perpendicular velocities; and $\gamma = [1 - v^2/c^2]^{-1/2}$. The radiation intensity at the nth harmonic for a free electron in a steady magnetic field is (in mks units)[5]

$$I_n(\omega, \theta) \, d\Omega = d\Omega \, \frac{e^2 \omega^2}{8\pi^2 c \, \epsilon_0} \left[\left(\frac{\cos \theta - \beta_\|}{\sin \theta} \right)^2 J_n^2 \left(n\beta_\perp \, \frac{\sin \theta}{1 - \beta_\| \cos \theta} \right) \right.$$

$$\left. + \beta_\perp^2 \, J_n'^2 \left(n \, \beta_\perp \, \frac{\sin \theta}{1 - \beta_\| \cos \theta} \right) \right] \left\{ \delta[n\omega_c - \omega] \right\} \,,$$

$$(2)$$

where J_n and J_n' denote the Bessel's function of the first kind and its derivative with respect to its argument. The delta function shows that the radiation occurs only at the fundamental cyclotron frequency and harmonics. For propagation perpendicular to the magnetic field the first term ($\sim J_n^2$) in Eq. 2 accounts for the ordinary wave, which is polarized with its electric vector parallel to the magnetic axis, while the second term ($\sim J_n'^2$) accounts for the extraordinary wave with

E ⊥ to B. The ordinary wave amplitude is always small compared to the extraordinary wave amplitude. For parallel propagation ($\theta = 0$) and a two-dimensional Maxwellian, radiation occurs only at the fundamental frequency.

The frequency spectrum of the synchrotron radiation at a given angle is obtained by integrating the Schott-Trubnikov formula (Eq. 2) over the velocity distribution, and summing over harmonics. These integrations were performed, using analytic approximations, by Trubnikov[3] and numerically by Beard and Baker[5] and Hirshfield, Baldwin, and Brown.[6] The theoretical spectra of synchrotron radiation, which we use to compare with experimental results, are obtained by numerical integration, similar to that of Beard and Baker, of the product of Eq. 2 (with $v_{\parallel} = 0$) and a two-dimensional Maxwellian distribution

$$f(U) = \frac{U + E_0}{kT(E_0 + kT)} e^{-U/kT} , \qquad (3)$$

where U is the kinetic energy, $U = E_0(\gamma - 1)$, and $E_0 = m_0 c^2$.

The total radiation at any angle can be found if Eq. 2 is integrated with respect to frequency. For $\theta = 90°$ the result is

$$I_{\perp} \, d\Omega = \left[\frac{c^3 e^4 B^2}{128 \pi^2 \epsilon_0 E_0^5} \right] \left[\frac{U(U + 2E_0) \left[7(U + E_0)^2 - 3E_0^2 \right]}{U + E_0} \right] .$$

The total radiation in watts per steradian per electron is

$$P_\perp \, d\Omega = d\Omega \int_0^\infty I_\perp(U) \, f(U) \, dU$$

$$= \frac{d\Omega \, e^4 \, c^3 \, B^2}{128\pi^2 \, \epsilon_0^2 \, E_0^2} \, \frac{\alpha}{\alpha+1} \left[8 + 64(1/\alpha) + 168(1/\alpha)^2 + 168(1/\alpha)^3 \right], \quad (4)$$

where $\alpha = E_0/kT$ and $f(U)$ is the two-dimensional Maxwellian of Eq. 3.

For $\theta = 0$, the integration of Eq. 2 (with $v_\parallel = 0$), with respect to frequency and over the two-dimensional Maxwellian, yields

$$P_\parallel \, d\Omega = \frac{d\Omega \, e^4 \, B^2 \, c^3}{16\pi^2 \, \epsilon_0^2 \, E_0^2} \, \frac{\alpha^2}{1+\alpha} \, e^\alpha \left\{ E_1(\alpha) - E_3(\alpha) \right\}, \quad (5)$$

where $E_1(\alpha)$ and $E_3(\alpha)$ are exponential integrals

$$E_1(\alpha) = \int_1^\infty (1/t) \, e^{-\alpha t} \, dt \, ,$$

$$E_3(\alpha) = \int_1^\infty (1/t)^3 \, e^{-\alpha t} \, dt \, .$$

B. Absorption

As with the radiation calculation, we assume that the frequency of the radiation is sufficiently above the plasma frequency that the plasma is transparent and the rf wave interacts with single particles. Seidl[7] used a perturbation method to study this interaction for a

nonrelativistic charged particle in a magnetic mirror configuration. He found, within the assumptions, (1) that the unperturbed motion could be described by adiabatic constants and (2) that the rf perturbation of the particle energy is small in a longitudinal period, that the energy of most charged particles does not increase indefinitely in time but rather oscillates about an average value. In order to check the sensitivity of Seidl's results for cases that do not satisfy his assumptions, equations of motion for a charged particle were numerically integrated for the case of a magnetic mirror field and a circularly polarized plane wave propagating along the magnetic field.[8] The parameters were chosen so that cyclotron resonance occurs at some point between the minimum and maximum magnetic field. For cases of small excursion into a weak magnetic field gradient, Seidl's adiabatic approximation is shown to be valid by the numerical results. For a large excursion into the magnetic field gradient of a mirror region, even in the absence of an rf field, the magnetic moment may not be a constant of the motion. In this situation, in which Seidl's assumptions are violated, the energy of the electron is not periodic within the time limits of the numerical calculation, and some electrons lose enough transverse energy to escape via the mirror loss cone. These numerical results indicate that, in addition to the few particles that Seidl's theory predicts are heated, another class of particles, with large longitudinal excursions, undergo a significant change in their energy.

Experimental work on electron cyclotron heating within magnetic mirrors has been reported by Dandl et al.[9] and by Kuckes.[10] Their results, which indicated substantial heating, applied to situations in which the single particle theory is not adequate. In Dandl's work, collision processes were important. In Kuckes experiment, collective effects predominated. Both of their plasmas were created, as well as heated, by the rf. In the heating experiments reported here, the rf power is applied to an already hot electron plasma (5 - 20 keV) in which the single particle treatment is valid.

II. RADIATION EXPERIMENTS

A. Description of Apparatus and Measurement Techniques

The radiation spectrum emitted by the magnetically confined hot electron plasma has been studied in the wavelength region from 4 to 0.2 mm. To detect this radiation, a cryogenically operated indium-antimonide photodetector is used. This detector has a measured output of approximately 1.0 V/mW at 1 mm wavelength for the nominal conditions of detector operation (i.e., the indium antimonide crystal at a temperature of 1.7° K, with a bias current of 1 mA/cm^2 in a dc magnetic field of 6.4 kG). The response time of the detector is < 1 μsec. The spectral distribution of the radiation is measured with an echelette grating monochrometer. The bandwidth of the monochrometer is 10 % at the central frequency in each grating. The angular acceptance angle

is 0.1 steradian, which limits observations to plasma located near the midplane of the magnetic mirror. Five gratings are required to cover the region from 4 to 0.2 mm wavelength, and additional filters in the form of gratings, mesh filters, quartz windows, black photographic paper, and blackened polyethylene, are used to ensure that only the intended wavelength arrives at the detector. To determine the absolute intensity of radiation measured by the combined monochrometer-detector system, the radiation is compared with a secondary standard, ultraviolet, mercury arc lamp that has an equivalent blackbody temperature of approximately 3000° K between 2.0 and 0.2 mm wavelength. The mercury arc lamp is calibrated against a primary standard blackbody of 200° C. The low intensity of the standard sources requires synchronous detection. The long post-detection integration time for the primary standard prevents its use directly with the experiment. The total radiation emitted at all frequencies by the hot electron plasma is measured by operating the monochrometer in zero order, or by admitting the radiation directly into the detector. The radiation is guided to the monochrometer or detector by hollow metal light-pipes. The attenuation of these light-pipes is included in the evaluation of system sensitivity.

B. Experimental Results

The radiation emitted by the plasma is measured separately for propagation perpendicular to the magnetic axis in the midplane between the mirrors, and for propagation parallel to the magnetic field. In each of these locations, the total radiation and the spectral distribution of the radiation are measured. Results are given for each of these four situations.

Previously reported experimental results did not include measurements of radiation parallel to the magnetic axis or results with an absolute intensity calibration. Improved techniques for measuring the spectral distribution have revealed that in certain instances there is a two-peak structure in the emission spectrum which is most distinct on the fundamental.

Perpendicular Radiation Spectrum

The spectral distribution of radiation observed in the direction perpendicular to the magnetic axis is shown in Fig. 2(dark line), taken from data at the peak of the compression cycle with a midplane magnetic field of 50 kG. The curve is constructed from a composite of many separate spectral measurements, each measurement itself consisting of a normalized average of 3 to 9 shots at every point. There were significant differences in the spectrum for different runs, well

outside of the computed rms deviation. These differences which do not appear in the composite spectrum of Fig. 2, are discussed below. In the same figure we compare the measured spectrum with computed two-dimensional Maxwellian distributions at 75 and 100 keV, normalized to the experimental second harmonic amplitude. The general features of the measured spectrum are seen to agree with the calculated spectrum at the temperature, measured by X-ray pulse height analysis, of 75 keV. The synchrotron radiation appears to give a somewhat higher temperature, which is consistent with the fact that the X-ray pulse heights are measured during the millisecond after peak compression when the temperature is decreasing. The minima in the spectra between the first and second harmonic and between the second and third harmonic are quite close to the theoretical predictions, but the peaks of the first and second harmonic radiation are shifted to lower frequencies. This difference is at least partially accounted for by the appearance of secondary peaks in the spectra of certain runs, as discussed below.

Spectra have also been constructed for the radiation 1 msec after the peak compression, showing, generally, a shift to lower frequencies, and also showing a lower amplitude of the radiation which is attributed both to cooling and to the loss of particles. The shift to lower frequencies and part of the amplitude reduction is a result of the

decay of magnetic field strength together with the consequent adiabatic cooling of the plasma. In addition to this adiabatic cooling, there is radiation cooling which preferentially cools electrons in the tail of the Maxwellian distribution. A self-consistent calculation, using a Fokker-Planck equation with a radiation damping term, predicts a cooling rate of 2 keV/msec which is not sufficient to account for the observed cooling.[11] Neither the excess cooling nor the loss of particles can be accounted for by coulomb collisions with ions. The hot electrons have a large ionization cross section which produces burn-out of the initial burst of gas from the source. This is seen from observations of the visible and UV light spectrum which is initially high but becomes quite small late in time. It is not known whether the rate of evolution of gas from the walls is sufficient to cause the observed cooling and particle loss after peak compression.

On some runs the spectra show a splitting of the peak radiation both on the first and second harmonic, as shown for one particular run in Fig. 3. The lower frequency peaks correspond to a distinctly lower value of magnetic field. On the runs in which the lower frequency peaks were most distinct, the plasma also exhibited a low-frequency instability on many shots, resulting in a loss of hot electrons. The observed instabilities are discussed briefly in Sec. IV. Observations with the end-loss camera indicate that, on some shots, in

addition to the hot plasma core, there is a concentric shell of hot plasma. A photograph of this phenomenon is shown in Fig. 4. The core corresponds to a midplane plasma diameter of 4 mm, while the shell extends beyone a diameter of 1 cm. A model for the splitting of the synchrotron radiation harmonics can be constructed based on the existence of a plasma shell. A calculation assuming a 60 keV core and a 40 keV shell (with a diameter somewhat larger than that observed in the end-loss photographs) is compared with the experimental results in Fig. 3. Other explanations for the double peaks have also been considered, but none appear to give a fully consistent picture of the phenomenon.

Theory predicts that the radiation emitted perpendicular to the magnetic axis is polarized with its electric vector perpendicular to the magnetic axis. Measurements with ruled (1000 lines per inch) thin gold foil, failed to reveal any preferred polarization. It is suspected that polarization mixing in the light pipe system is responsible for this negative result.

Parallel Radiation Spectrum

The radiation spectrum for emission parallel to the magnetic field is strongly peaked at a frequency slightly less than the fundamental frequency ($\omega_0 = eB/m_0$). This is seen in Fig. 5 which shows the spectrum at the peak of compression and 1 msec after peak compression

for the same parameters as the perpendicular spectrum. Theory predicts no harmonic radiation, but the experiment does not completely satisfy the theoretical model. The presence of the small second and higher harmonic radiation is explained by the solid angle and magnetic field curvature. The fundamental is broader than for the perpendicular radiation. This is caused by Doppler broadening and by the fact that the parallel radiation originates from all magnetic fields between the mirrors and the midplane. The two-peak structure is also present in the parallel radiation spectrum presented here. The same model used for the perpendicular case of a hot core and slightly colder shell of plasma is used again to obtain the theoretical spectrum shown in the figure.

The spectrum 1.0 msec after peak compression gives a peak amplitude that is decreased by a factor of 2 from that at peak compression. This decrease is considerably larger than that expected from the adiabatic cooling, and from the nonadiabatic effects discussed in connection with the perpendicular radiation, and has not been explained.

Total Radiation

The total radiation either perpendicular or parallel to the magnetic axis can be measured as a function of magnetic field by two

methods. The first is to average the intensity at a particular peak magnetic field and then to change to a different peak compression field. The second is to measure simultaneously the time-dependence of the magnetic field and the synchrotron radiation and then to eliminate time to obtain radiation intensity as a function of magnetic field. Both methods give the same result; however, the data used here are from the second method, which is more convenient.

Figure 6 shows the total radiation both parallel and perpendicular to the magnetic axis as a function of time, together, with the time varying increase of the magnetic field. The average increase of the radiation intensity as a function of the increase of magnetic field strength can be expressed, within a small interval of field, as a power of the magnetic field. The average between 40 and 50 kG yields, for perpendicular radiation,

$$P_\perp \propto B^{3.82} .$$

From Eq. 4 it is seen that for a small interval in T there exists an approximate relation

$$P_\perp \propto B^2 T^{x_\perp(T)}$$

and consequently, with $x_\perp = 1.82$ from the observation an electron temperature of 70 keV is calculated. This method of deducing the plasma electron temperature is not as accurate as that obtained using

a full spectrum because it assumes a constant amplitude versus wave-length response of the indium-antimonide detector, ignores particle losses during compression, and is averaged over an interval in B. Despite these shortcomings, the estimate of temperature agrees generally with that obtained by other methods. An estimate of the total number of radiating particles is obtained from a comparison of the theoretical total power, at the above temperature and magnetic field, with the total measured power based on an average response of the detector of 0.5 V/mW. With this method, the total number of particles is of the order of 10^{11}. Together with the measurements of plasma volume using the end-loss camera, this given the plasma density, already quoted, of 10^{12} cm^3. The X-ray bremsstrahlung measurements have shown that the spread of plasma temperature is only a few percent. For this reason, the total synchrotron radiation is a convenient, relative density monitoring diagnostic, as well as an indirect method of measuring the absolute density.

The measured rate of increase of intensity of radiation emitted parallel to the magnetic axis as a function of the magnetic field strength is expressed as a power of the magnetic field,

$$P_{\parallel} \propto B^{(4.5 \pm 0.5)} = B^2 T^{x_{\parallel}}$$

such that $x_{\parallel} = 2.5 \pm .5$. This exponent is much larger than the theoretical value of $x_{\parallel} = 0.55$ obtained from Eq. 5 for a 70 keV plasma.

This discrepancy has not been completely resolved but the effect may also account for the major portion of the large decrease in the peak of the parallel radiation spectrum observed after the peak compression. One possible explanation involves the frequency response of the detector and light pipe system which is assumed to be flat in comparing theory and experiment. The absolute calibration, discussed in Sec. IIA, is not complete for wavelengths longer than 2 mm and may, in fact, fall off sufficiently to account for the discrepancy.

III. ABSORPTION EXPERIMENTS

A. Description of Apparatus

To study the electron cyclotron resonance heating of an already hot electron plasma, short pulses of rf power at 3 cm and at 8.0 mm wavelengths are applied. A 250-kW magnetron, with a pulse length of 0.5 μsec, supplies linearly polarized 3 cm power. A 100-kW magnetron, with a 2.0-μsec pulse length supplies 8 mm rf power in a TE_{01} mode with a zero field intensity on axis. The rf energy at each wavelength is fed into the vacuum system either parallel or perpendicular to the magnetic field. The experimental sequence and diagnostic instrumentation are the same as for the emission experiments except for the addition of the magnetron pulses. The time at which the magnetron is pulsed is varied over a wide range that includes

those times which correspond to resonance at the peak of the mirror and at the midplane. The magnetron is also pulsed at times earlier and later to investigate any heating that might occur away from the resonant condition.

B. Results

Electron cyclotron resonance with the 3 cm rf power will occur at a magnetic field of 3.6 kG. The time at which the midplane magnetic field attains this value is 42 μsec after the start of the compression cycle. For 8 mm radiation the resonance at the midplane magnetic field of 12.5 kG corresponds to a time of 95 μsec after the start of the compression cycle. These times are shown in Fig. 7 as dashed lines on a plot of the midplane magnetic field as a function of time. Resonant interaction with the magnetic field, somewhere within the mirror, will occur at times below the corresponding dashed lines in each of the two cases.

3 cm Radiation

In Fig. 8, the total synchrotron radiation is compared with and without 3 cm rf heating. There is a large enhancement of the synchrotron radiation signal if rf heating is applied during the period when electron-cyclotron resonance occurs between the mirror peak and the mirror midplane. In Fig. 9, the integrated pulse-height

-17-

distribution of bremsstrahlung X-rays are given for 3 cm rf power pulsed at various times both before and after the optimum time for resonance heating. The time of 37 μsec shows the greatest heating with the apparent bulk of the heating occurring at the higher temperatures. The increase in the synchrotron radiation signal due to this temperature increase, as calculated from Eq. 4, is only a small part of the experimentally observed increase in radiation. We are thus led to believe that the rf pulse increases the plasma density by ionizing and heating neutral gas in the vacuum chamber.

Figure 10 shows the X-ray pulse-height distributions for radiation propagated parallel to the magnetic axis. These distributions are compared with distributions for 40 and 50 kG without the rf. The heating for this situation is less than that for perpendicular incidence, and at 32 μsec there is apparent cooling of the plasma.

8 mm Radiation

In Fig. 11, a comparison is made of the X-ray bremsstrahlung pulse-height distribution with and without 8 mm radiation propagated perpendicularly to the magnetic field. For this case, the magnetron definitely reduced the plasma temperature. This cooling is tentatively attributed to the spatial distribution of the electromagnetic field which is such that the velocity of the electrons parallel to the magnetic field causes the electrons to pass through an rf field that reverses direction

in a short distance. Under some conditions this situation can result in a transfer of energy from the electrons to the wave.

In Fig. 12, a comparison is made of the X-ray pulse-height distribution with and without rf heating for parallel radiation. The times at which the rf energy was applied were chosen to correspond to times when resonance is possible. At 95 μsec the maximum increase (about 20%) in plasma temperature occurs. For this case, the enhancement of synchrotron radiation can be explained by the 20% increase in the plasma temperature. This indicates that, for these conditions, no additional hot plasma is created by ionization of the background gas.

C. Comparison with Single Particle Theory

Qualitatively, the experimental results confirm certain aspects of the single particle calculations. No significant heating of the bulk of the plasma was observed. In some cases a few electrons were subjected to a large increase in energy, as observed by the change in the tail of the pulse-height distribution. One contribution to these high-energy electrons comes, in some cases, from the few electrons that remain in resonance with the high-frequency field, as described by both the analytical and numerical calculations. Probably the greater contribution comes from those electrons penetrating more deeply into the mirror which, according to the numerical calculation, can have substantial energy excursions.

IV. OBSERVATIONS OF COOPERATIVE EFFECTS

In addition to the noncoherent radiation and the single particle absorption, a number of cooperative phenomena have been observed and are being investigated. We here briefly describe these effects without detailed analysis. At least three distinct types of instabilities have been recorded: two types result in loss of all or part of the hot electrons but not accompanied by microwave radiation, and the other type generates short pules of microwave radiation, but without appreciable loss of plasma particles. All of these instabilities have been observed from measurements of the total radiation between 8 mm and 0.2 mm, using the InSb detector, and corroborated with other diagnostics. Figures 13 through 15 are plots of the total radiated power within this wavelength range.

Of the two types of instabilities causing loss of hot electrons, one previously reported on[1] is shown in Fig. 13. It is characterized by a slow loss of the entire hot plasma, and is more likely to occur at higher plasma densities. There is a definite onset with increasing magnetic field, as seen in the figure. During the decay of the hot electron plasma, particles are observed to leave the plasma radially and the loss along field lines is enhanced. There is no accompanying radiation in the 8-mm to 0.2-mm range.

In Fig. 14 a relatively sharp drop in the total radiation indicates another instability, usually occurring during the decaying magnetic field, which dumps some, but not all, of the hot electrons radially to the walls. This instability characteristically is triggered by an external signal, and the 8-mm magnetron radiation proved to be an efficient trigger, provided the density was higher than some fixed value. This instability, similar to that previously discussed, is not accompanied by microwave radiation; the spike of radiation in the figure is accounted for by scattering from the 8-mm magnetron radiation.

In Fig 15 the total radiation between 8 mm and 0.2 mm includes instability radiation. These radiation bursts occur characteristically on the rising portion of the magnetic field. They occur more frequently and with larger magnitude on the shots with larger density, and could often be triggered and amplified in intensity by the 8-mm magnetron that was used in the heating experiments. Spectrometer measurements indicate that the frequency of the intense radiation corresponds primarily with the midplane electron cyclotron frequency at the time of occurrence. From the background synchrotron radiation one can deduce that there is no substantial loss of plasma.

The instability resulting in microwave radiation is most likely of the velocity-space type. Similar, though not necessarily identical, instabilities have been reported, for hot electron plasmas, by Perkins

and Barr[12] and by Ard et al.[13] The other two instablities are not of this type and are probably associated with low-frequency oscillations. Low-frequency instabilities have been observed experimentally in hot-electron plasmas, at lower magnetic fields, by a number of investigators.[13] Although flute-type growth, characteristic of the low-frequency instabilities, has not been observed in our experiments at high field strengths, we have observed the $m = 1$ mode under certain conditions when the peak compression field was reduced to approximately 10 kG.

ACKNOWLEDGMENT

REFERENCES

1. A. J. Lichtenberg, S. Sesnic, A. W. Trivelpiece and S. A. Colgate, Phys. Fluids 7, 1549 (1964).

2. F. H. Coensgen, W. F. Cummins, and A. E. Sherman, Phys. Fluids 2, 230 (1959).

3. B. A. Trubnikov and V. S. Kudryavtsev, Proc. Second Conf. on Peaceful uses of Atomic Energy.

4. W. E. Drummond and M. N. Rosenbluth, Phys. Fluids 3, 45 (1960).

5. D. B. Beard and J. C. Baker, Phys. Fluids 3, 45 (1960).

6. J. L. Hershfield, D. E. Baldwin, S. C. Brown, Phys. Fluids 4, 198 (1961).

7. M. Seidl, J. Nucl. Energy C 6, 597 (1964).

8. D. Tuma and A. J. Lichtenberg, J. Nucl. Energy (to be published).

9. R. A. Dandl., A. C. England, W. B. Ard, H. O. Eason, M. C. Becker, and G. M. Haas, Nuclear Fusion 4, 344 (1964).

10. A. F. Kuckes and L. A. Farrari, Am. Phys. Soc. Series II 11, 582 (1966).

11. A. J. Lichtenberg and D. Tuma, Phys. Fluids 8, 1405 (1965).

12. W. A. Perkins and W. L. Barr, Observation of a Velocity-Distribution Instability, UCRL 12434 Preprint (1965).

13. W. B. Ard, R. A. Dandl, and R. F. Stetson, Phys. Fluids 9, 1498 (1966).

washer stack
plasma source

trapping coil

main compression coil

bias field coil

main tube

28"

44"

4"

12"

gate valve

cold trap

diffusion pump
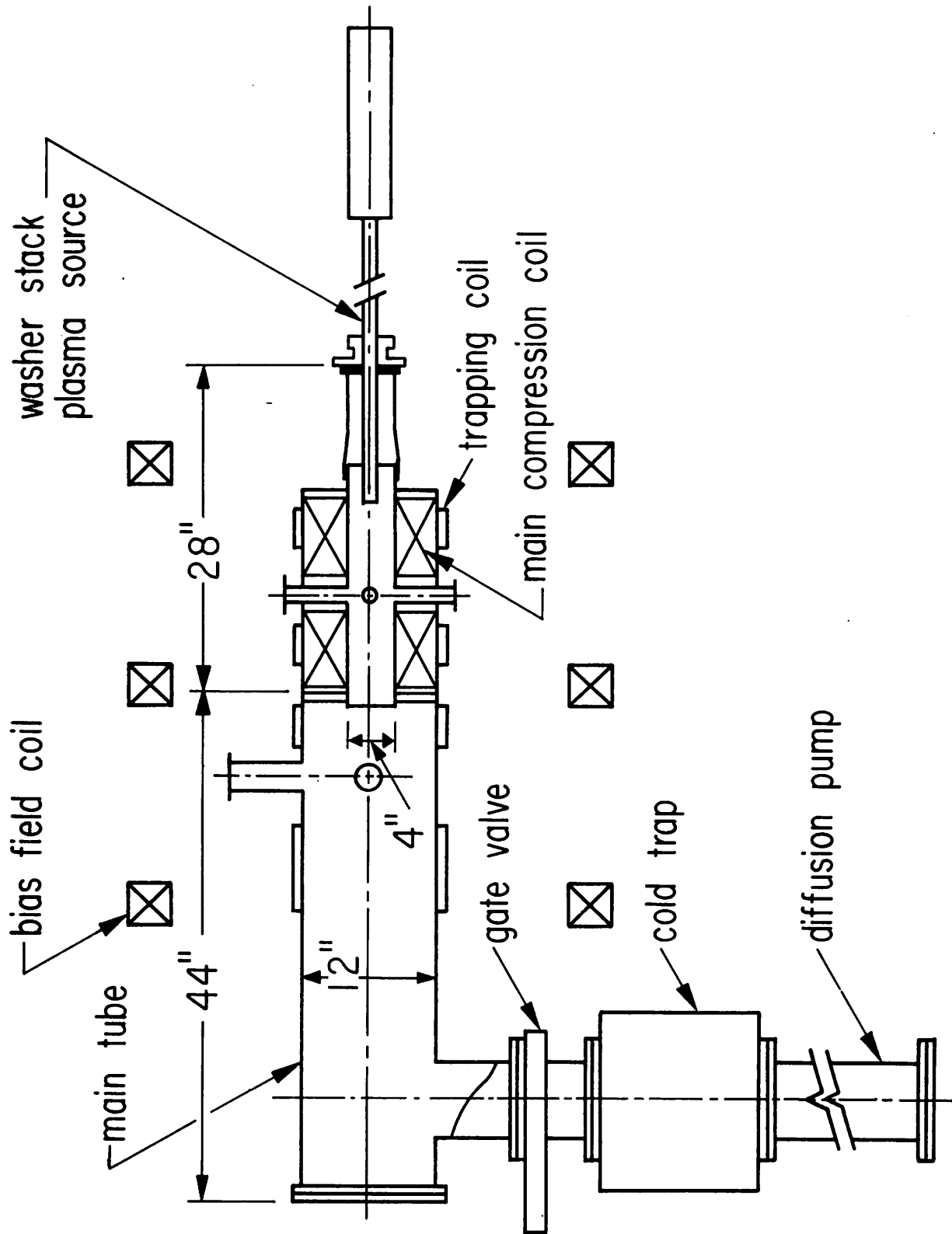
Fig. 1. Schematic layout of mirror machine.
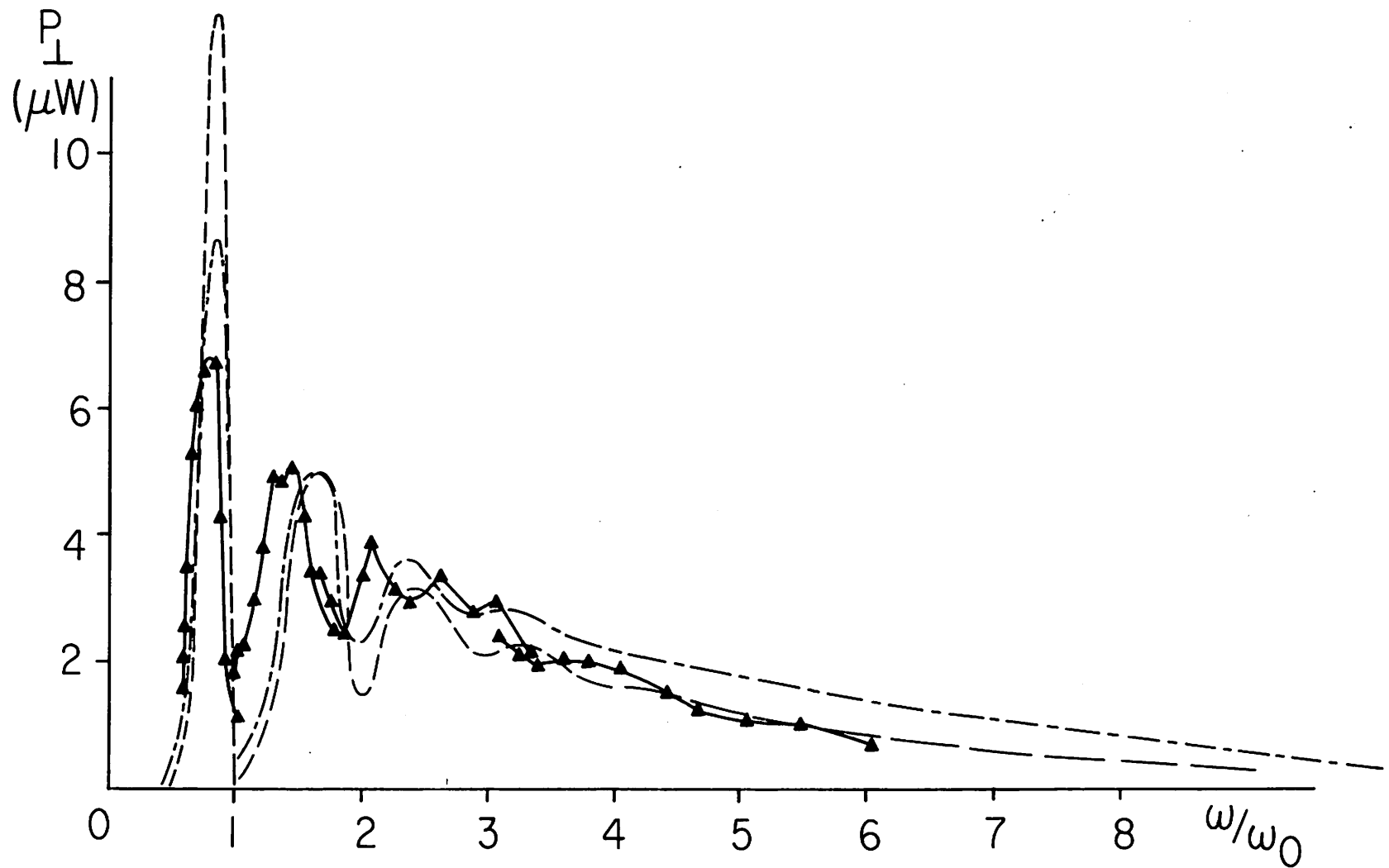
Fig. 2. Comparison of theory and experiment for the absolute power spectrum of perpendicular radiation in bandwidth $\Delta\omega$ and solid angle $\Delta\Omega$. For experiment: B = 50 kG on axis at midplane, $\Delta\omega = 0.1\,\omega_0$, $\omega_0 = eB/m$.

$\Delta\Omega = 0.1$ ster.; theoretical spectra are obtained from two-dimensional Maxwellian with radiation amplitude normalized to experimental second harmonic peak.
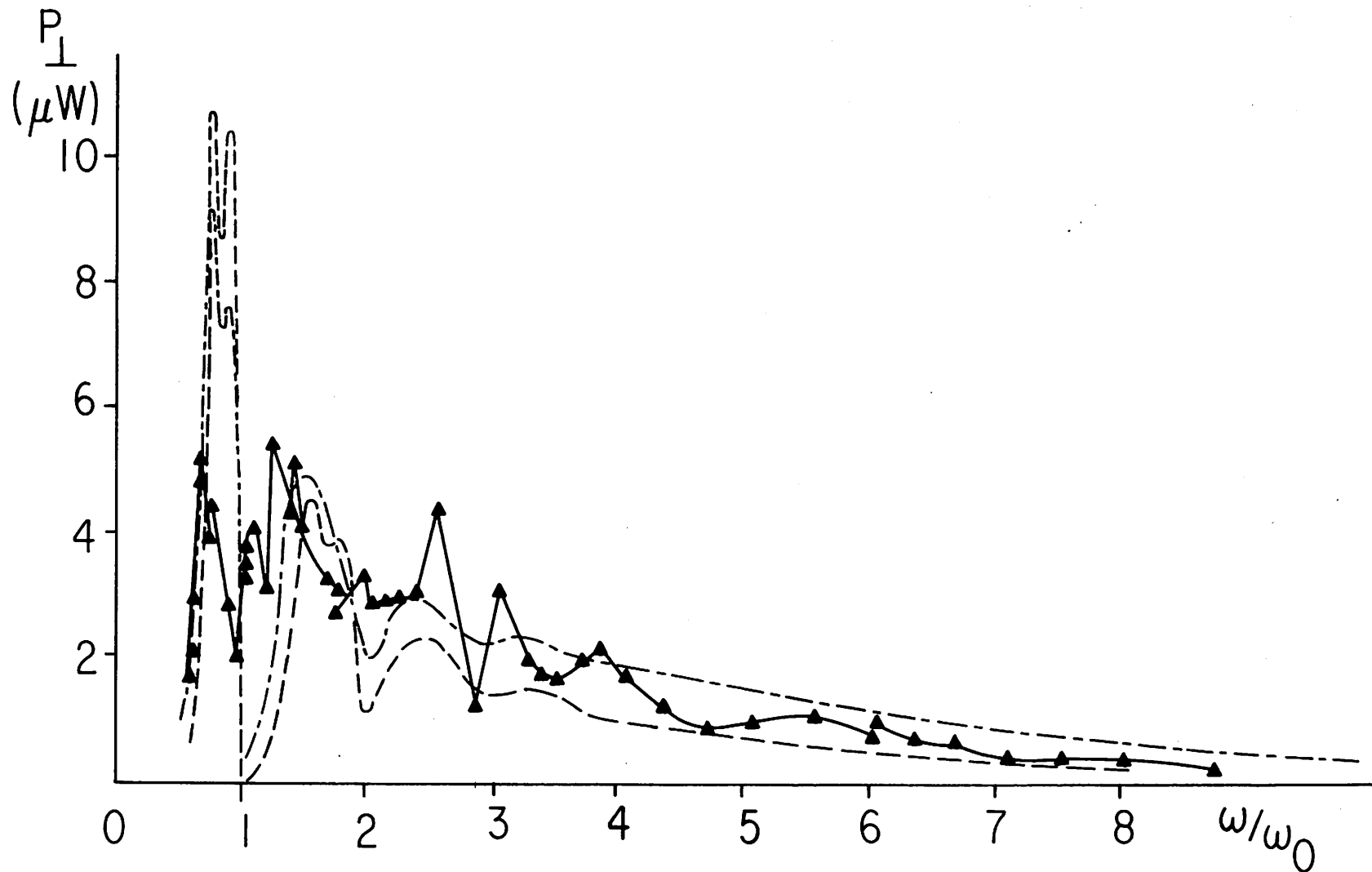
Fig. 3. Comparison of experimental results showing two peaks, with theoretical core-shell model. For theory core parameters are: B_c = 50 kG, kT_c = 60 keV; and the shell parameters are: B_{sh} = 42.5 kG, kT_{sh} = 40 keV, N_{sh} = 0.5 N_c, where N is total number of radiating electrons. Experimental parameters and normalization as in Fig. 2.
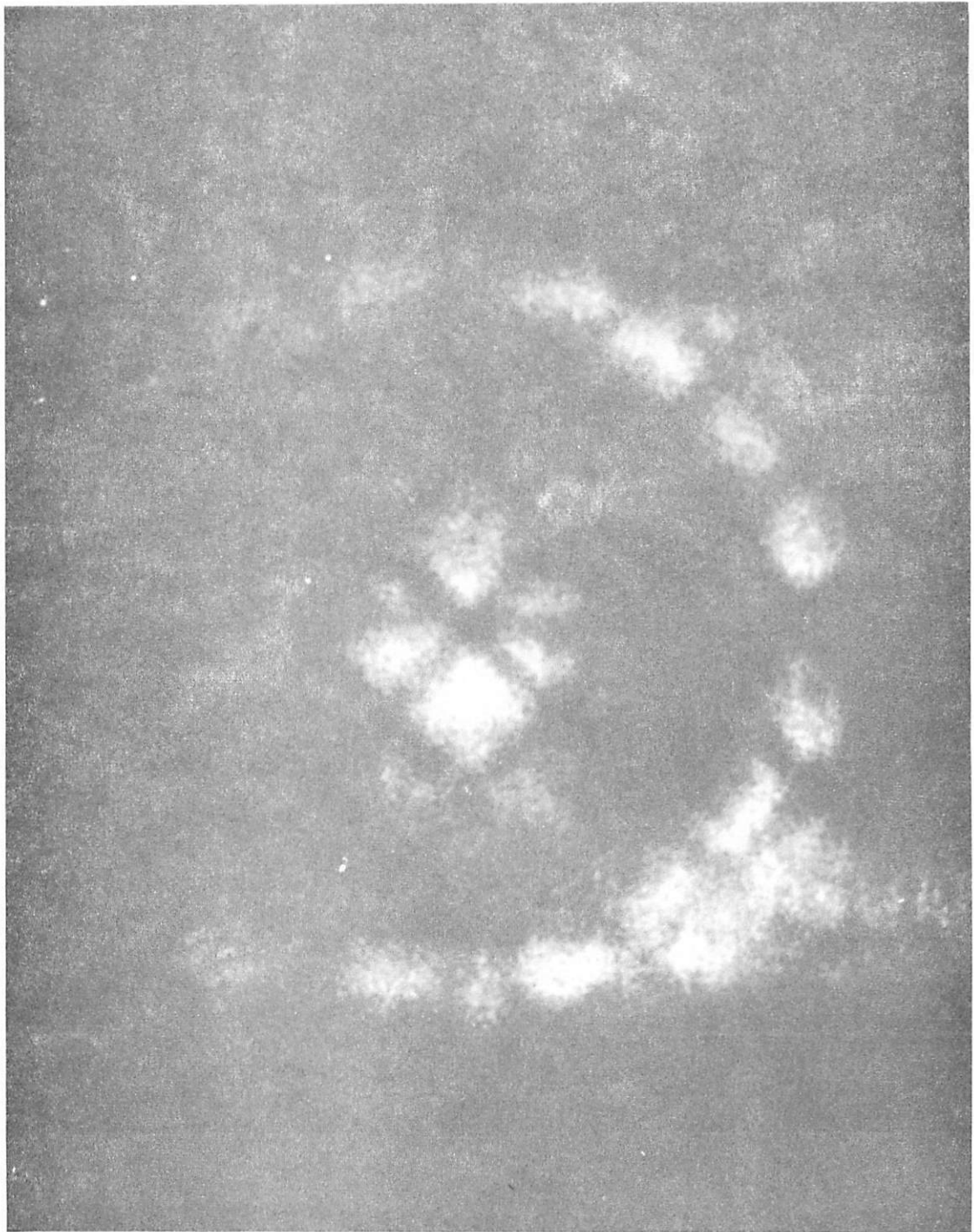
Fig. 4. Plasma camera photograph showing plasma
core and surrounding shell.
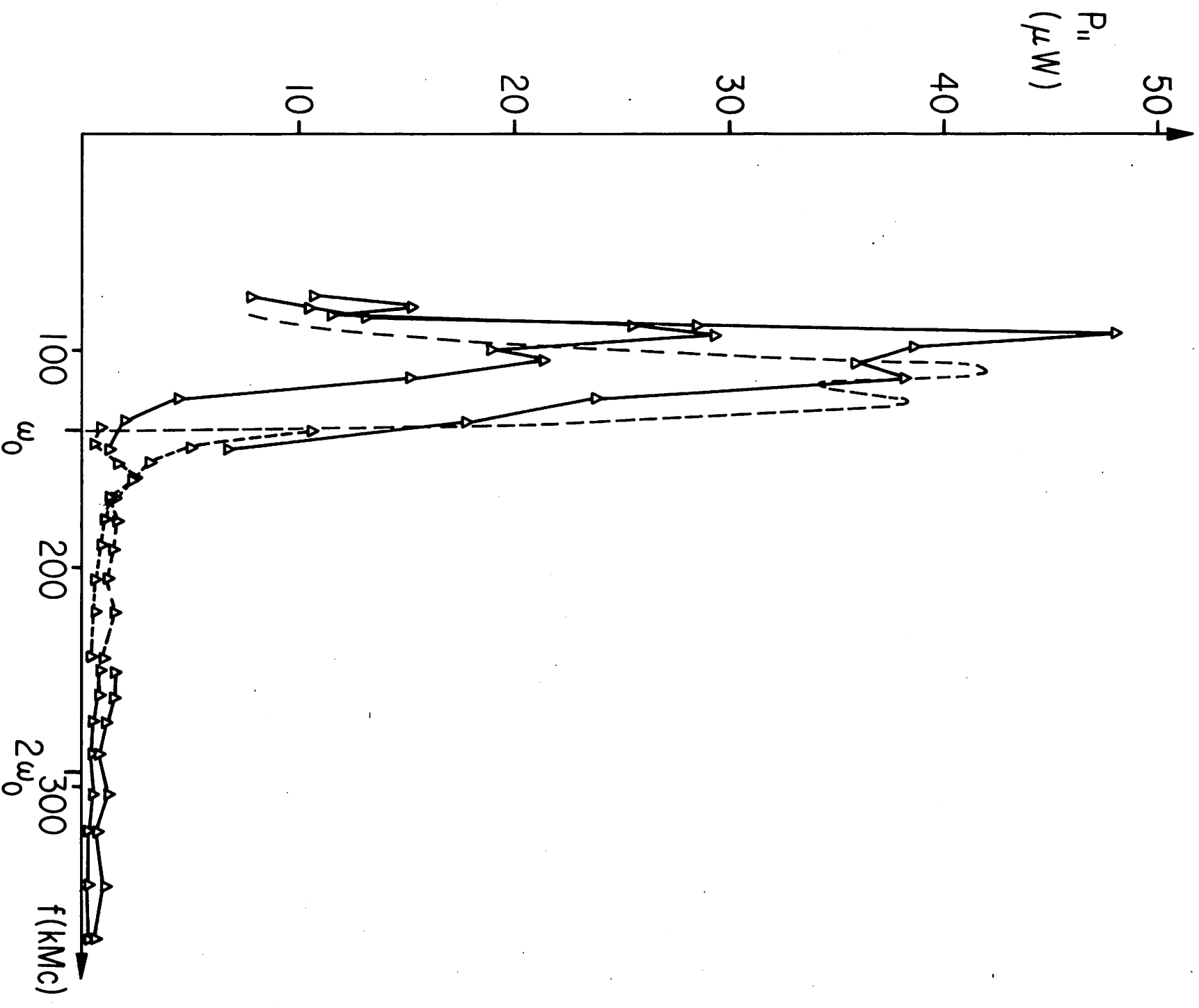
Fig. 5. Comparison of absolute power spectra for parallel radiation from experiment and theory. Theoretical parameters as in Fig. 3; experimental parameters and normalization as in Fig. 2 except that experimental spectrum 1 msec after peak compression is also given.
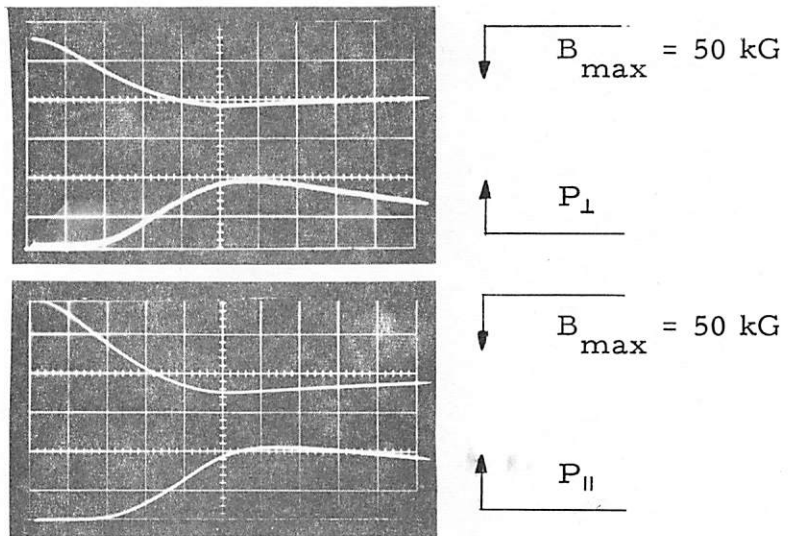
Fig. 6. Comparison of time variation of total synchrotron
         radiation perpendicular and parallel to magnetic
         field with the time variation of the magnetic field.
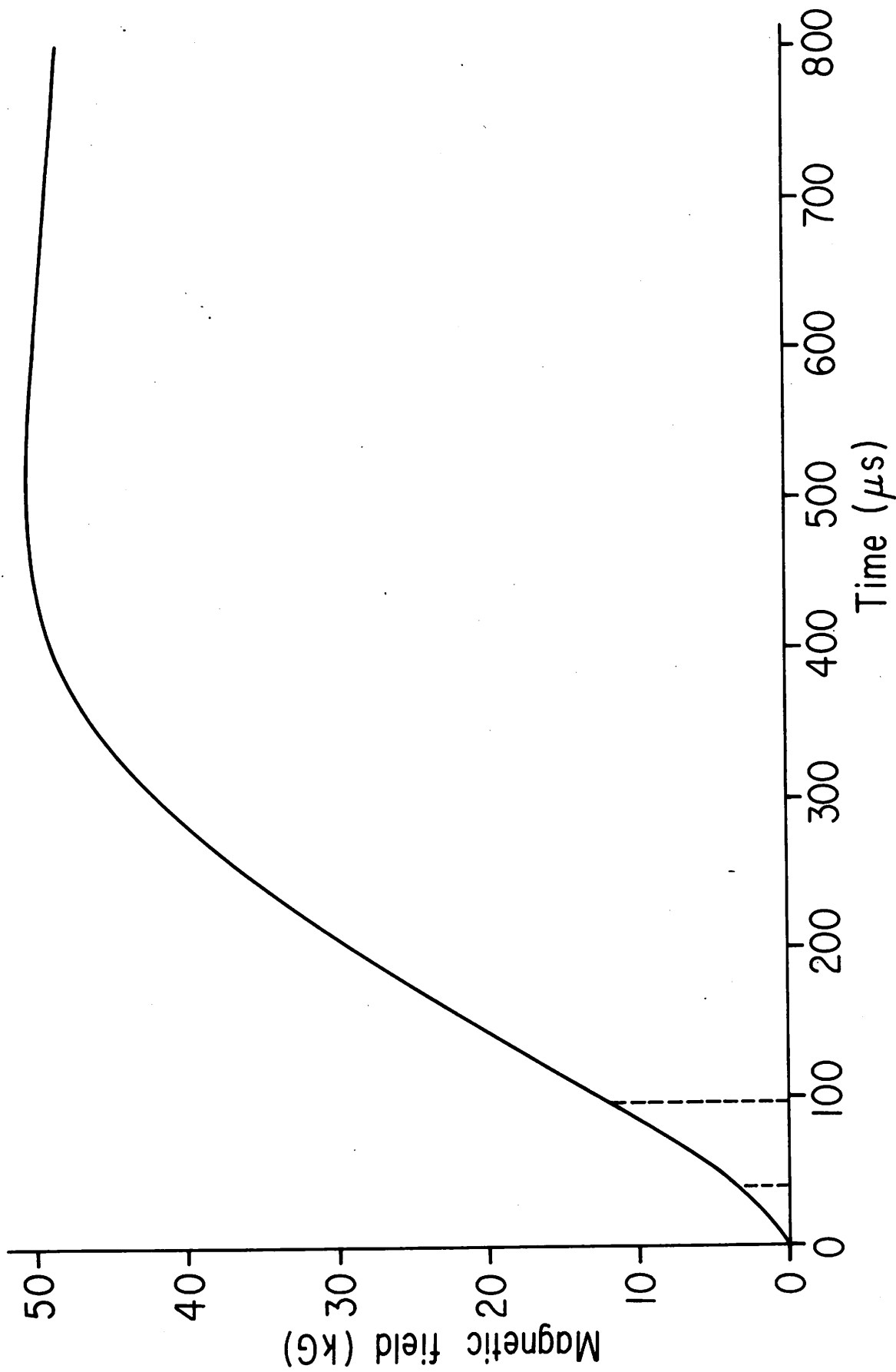
Fig. 7. Variation of the midplane magnetic field with time, indicating values of magnetic field for cyclotron resonance with microwaves of 3 cm and of 8 mm wavelengths. This field variation applies to all data in Figs. 8 - 12 in which pulsed rf energy is applied.
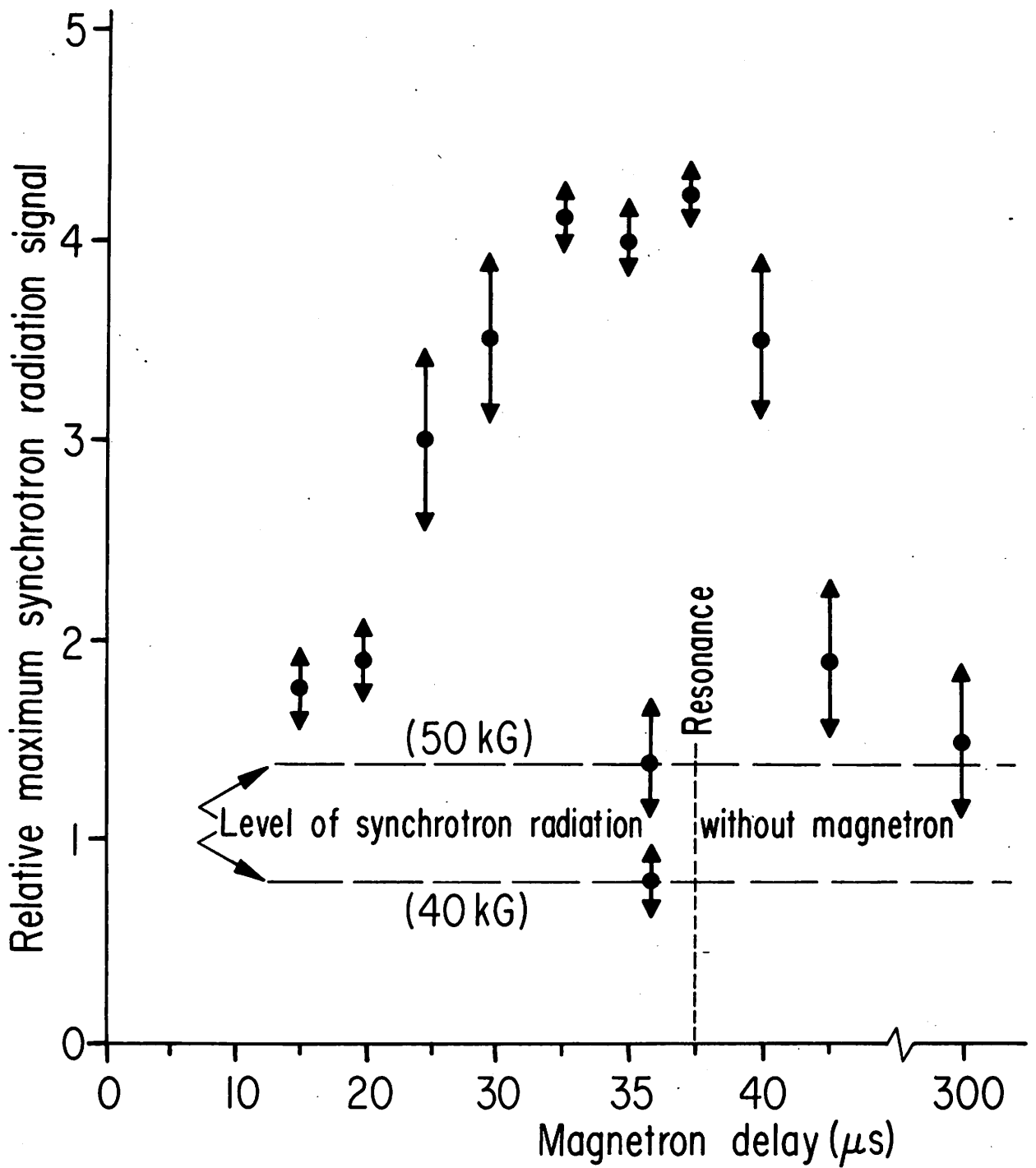
Fig. 8. Comparison of the synchrotron radiation for 40 kG and
50 kG maximum midplane magnetic field, with the synchrotron
radiation at 50 kG if pulses of 3 cm rf energy are propagated
perpendicular to the magnetic field at the times shown.
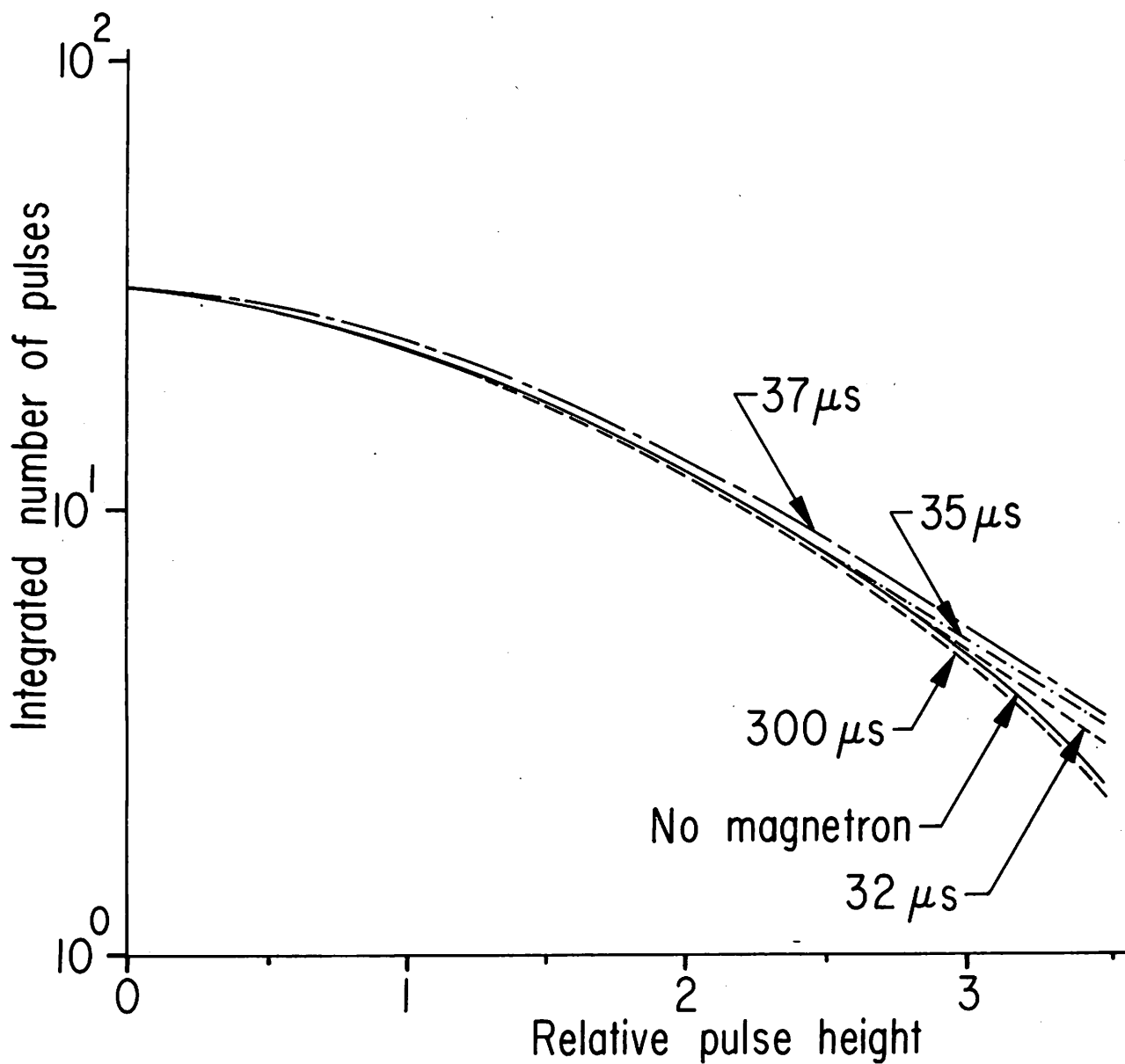
Fig. 9. Comparison of pulse height distributions of the plasma bremsstrahlung X-rays with and without 3 cm rf energy propagated perpendicular to the magnetic field. The pulse heights are counted for one millisecond following peak compression.
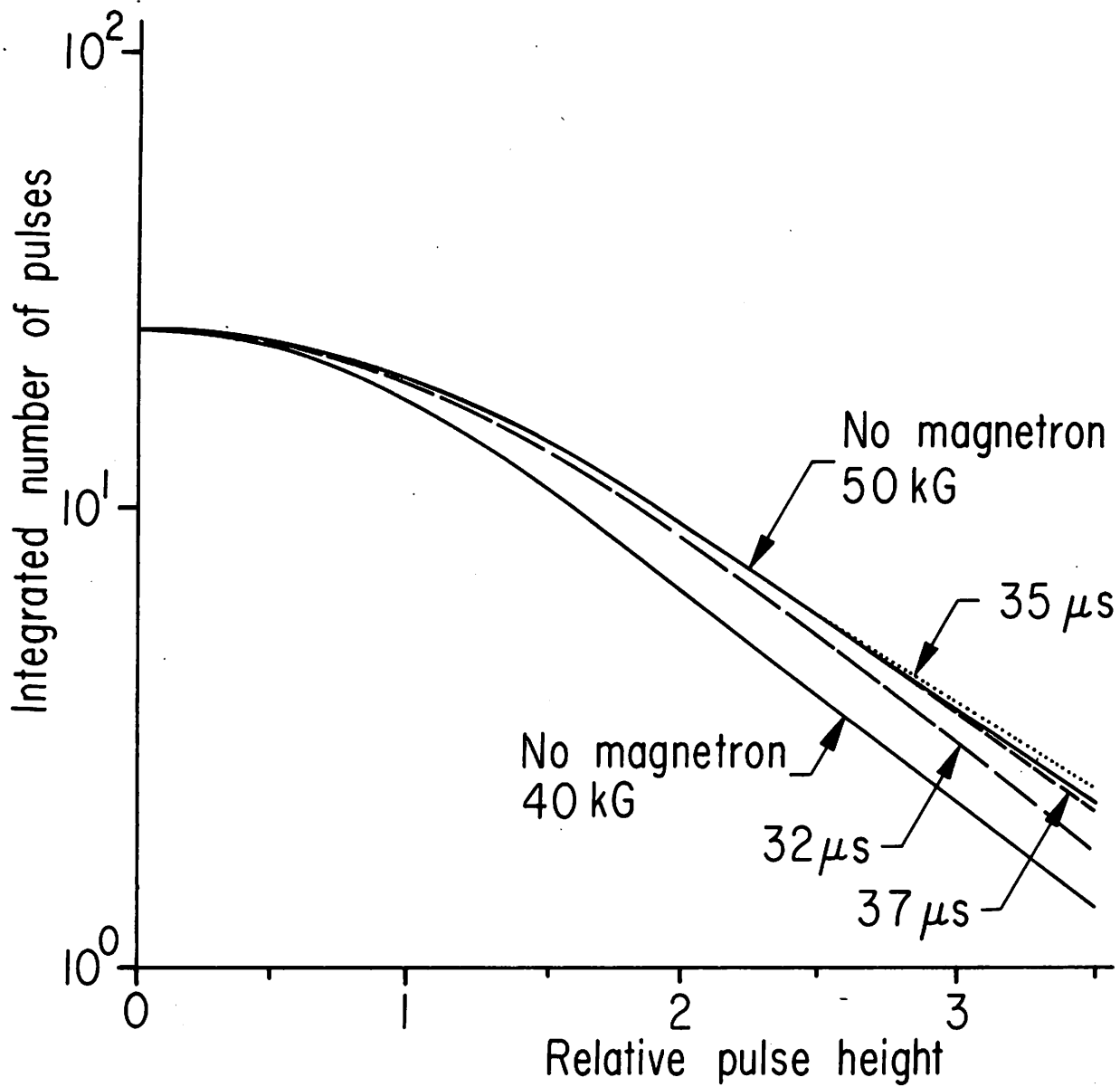
Fig. 10.   Comparison of the pulse height distribution of
bremsstralung X-rays at 40 kG and 50 kG magnetic
field, with results at 50 kG maximum midplane
field with 3 cm rf energy pulsed parallel to the field.
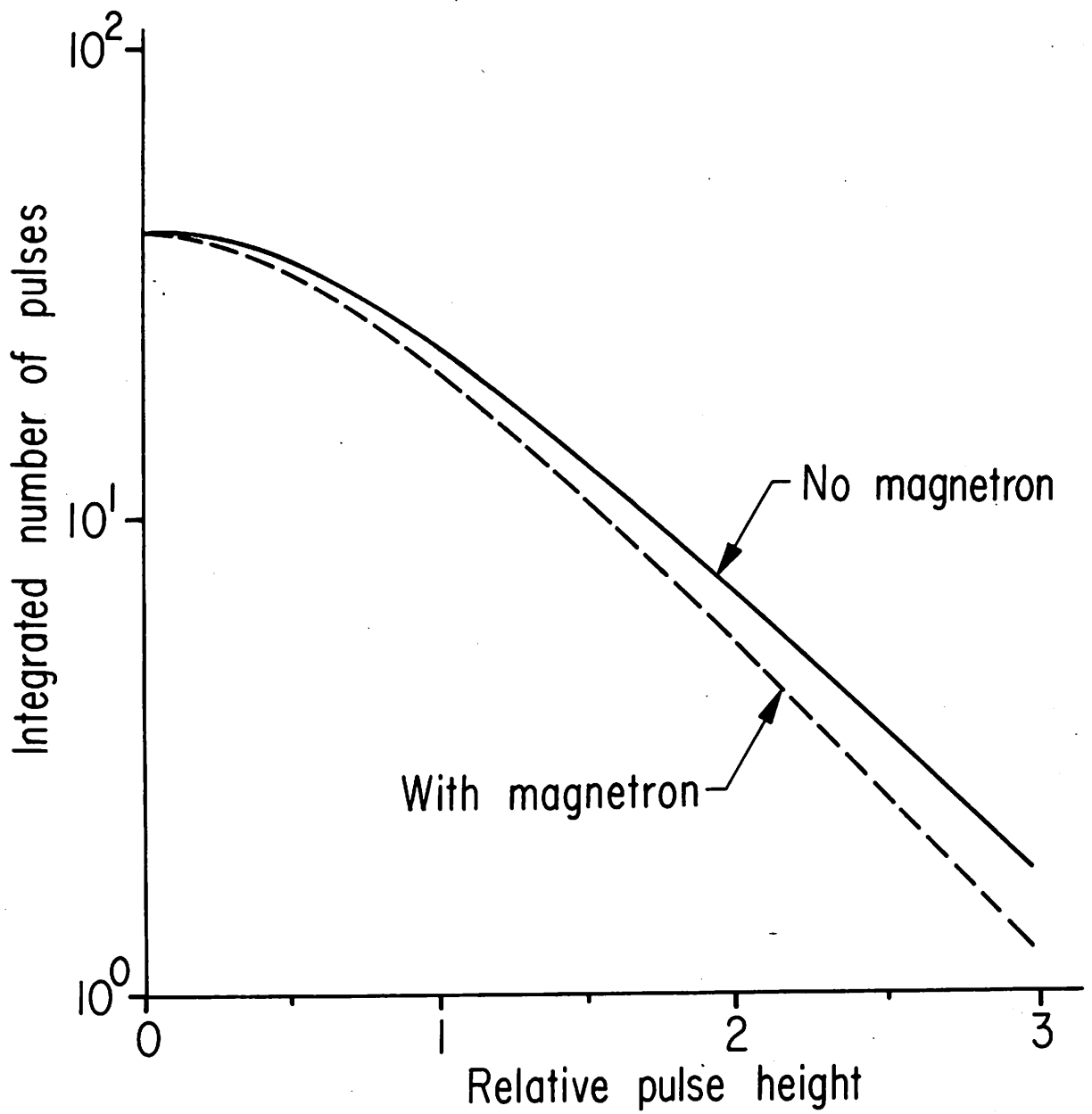
Fig. 11. Comparison of X-ray pulse heights with and without
rf energy pulsed perpendicular to the magnetic field.
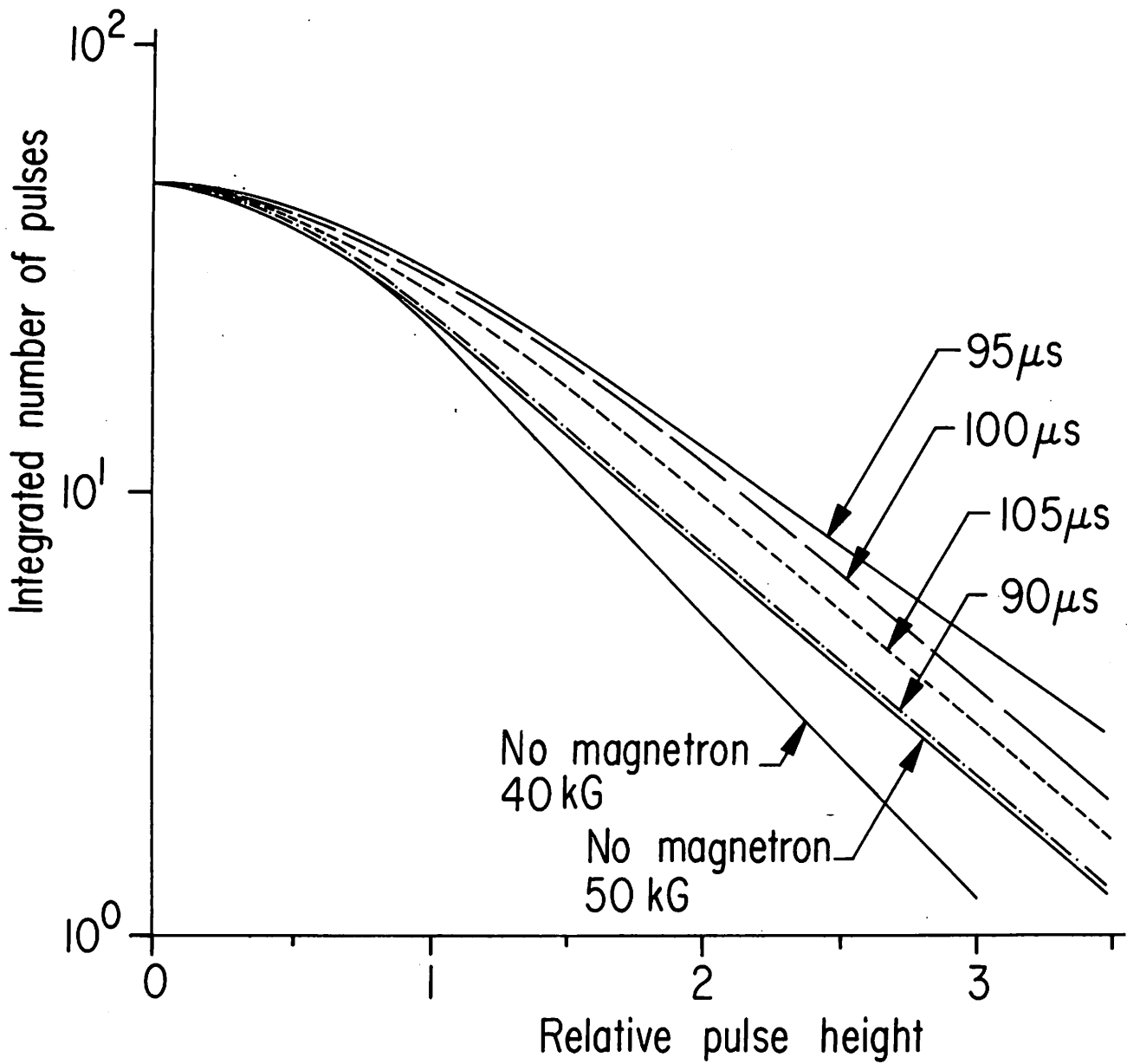
Fig. 12. Comparison of X-ray pulse heights without rf energy for 40 kG and 50 kG maximum midplane magnetic field, and with 8 mm rf energy pulsed parallel to the magnetic field for 50 kG magnetic field.
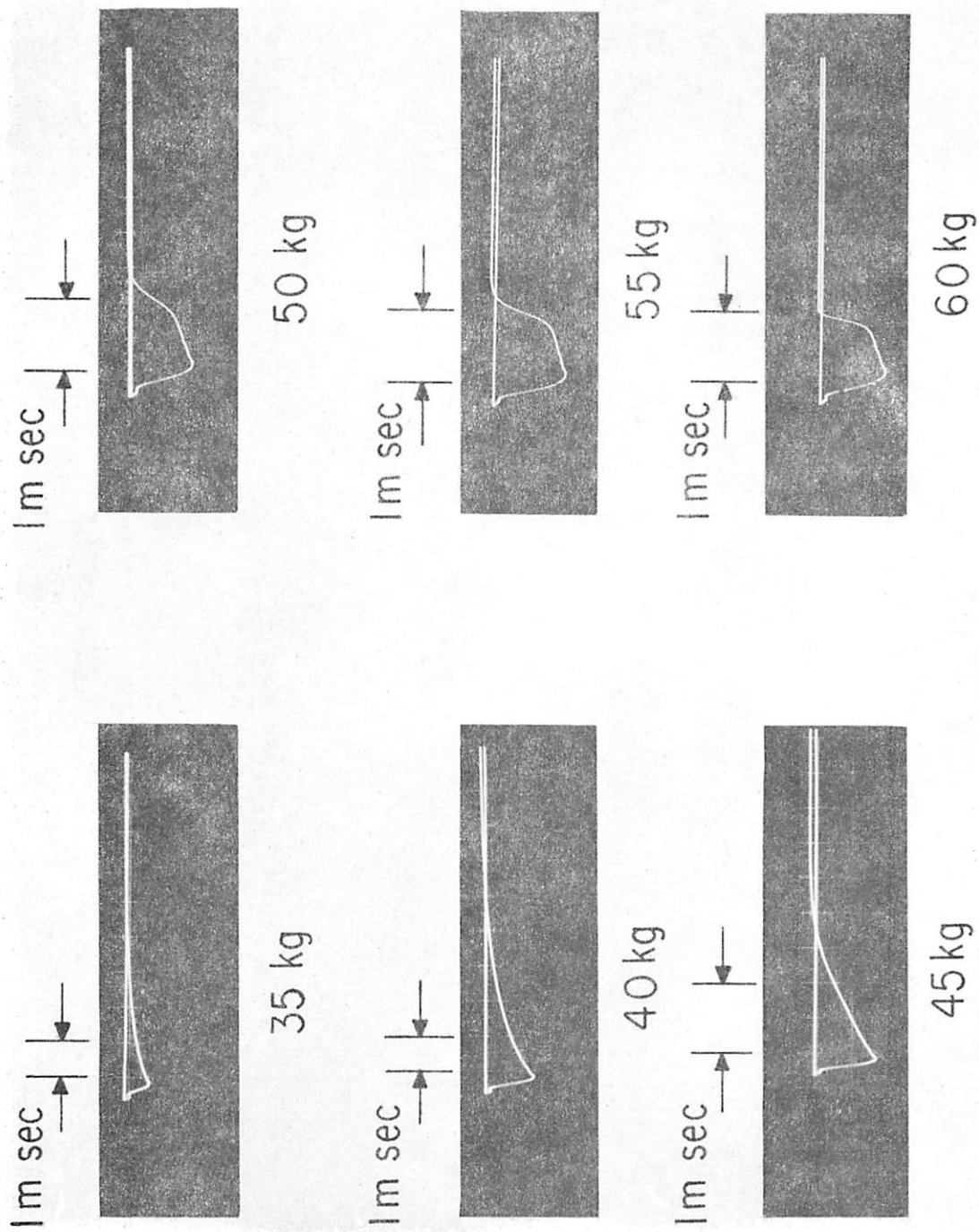
Fig. 13. Variation of synchrotron radiation with peak magnetic field indicating onset of instability with increasing field.
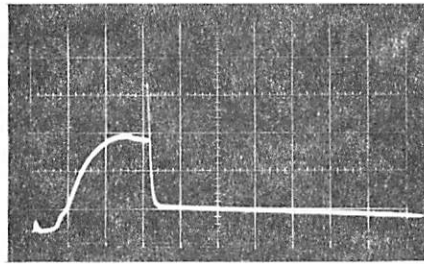
→| 1 ms |←

Fig. 14. Triggered instability which dumps
most, but not all, of the plasma.
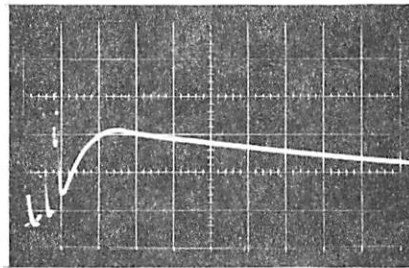
→| 1 ms |←

Fig. 15. Velocity space instability.